Impact formation and microstructure characterization of thermal sprayed hydroxyapatite/titania composite coatings

H. Li[a], K.A. Khor[a],*, P. Cheang[b]

[a] School of Mechanical and Production Engineering, Advanced Materials Research Centre (AMRC), Nanyang Technological University, 50 Nanyang Avenue, Singapore 639798, Singapore
[b] School of Materials Engineering, Advanced Materials Research Centre (AMRC), Nanyang Technological University, 50 Nanyang Avenue, Singapore 639798, Singapore

Abstract

Formation mechanism of hydroxyapatite (HA)/titania (TiO_2) composite coating deposited by high velocity oxy-fuel (HVOF) thermal spray process was studied, and its structural characterization was conducted and elaborated in this paper. The impact theory was employed to analyze the formation procedure of the HA/titania composite coatings. Results revealed that the crater caused by the impact of entirely unmelted TiO_2 particles on the HA matrix during coating formation was of smaller dimensions than the original size of the reinforcements. It was found that chemical reaction between the mechanically blended HA and TiO_2 powder took place exclusively during the impingement stage, and calcium titanate, $CaTiO_3$, was one notable by-product. The bonding between the HA matrix and TiO_2 reinforcement might have been achieved predominantly through a chemical bond that resulted from the mutual chemical reactions among the components. Differential scanning calorimetry analyses showed that the chemical reaction between HA and TiO_2 was at $\sim 1410°C$. The TiO_2 addition was found to exert particular effects on the thermal behavior of HA at elevated temperatures, during both heating and cooling cycles. Transmission electron microscopy observation identified the chemical reaction zone between HA and TiO_2, which revealed an improved splats' interface. The reaction zone demonstrated some influence on the grain size of HA nearby during resolidification of the melted portion. A structural model was proposed to illustrate the location of the different phases in the HA/titania composite coating.

1. Introduction

Hydroxyapatite (HA) is known for its bioactivity and, is widely used as an implant material in clinical applications. However, its utilization is severely limited by its intrinsic poor mechanical properties, which can lead to the discomfort of instability and substandard duration of the implant in the presence of body fluids, and local loading as compound stresses are generally experienced [1]. Even though the metallic substrate possesses high strength, prosthesis failure inadvertently occurs within thermal sprayed HA coatings [2,3] or at the coating/substrate interface [4]. The incorporation of bioinert ceramics as reinforcement within the coating was believed to be a way to improve the mechanical

reliability of the HA matrix [5–7]. It has been found that the addition of glass into HA had a major effect on the HA structure [8] and a positive effect on HA properties has also been reported [9,10]. The altered structure triggered by the bioceramic incorporation is believed as a direct factor responsible for the improved coating properties.

The addition of titania particulates to HA coating has attracted considerable attention [11–13], based on the assumption that titania is capable of enhancing osteoblast adhesion [14] and inducing cell growth [15]. However, to date, the knowledge of HA-based composite coating is still inadequate. The reinforcing mechanism of the secondary phase in HA matrix has yet to be convincingly disclosed. Generally, the reinforcing effect for thermal sprayed composite coatings can be attributed to either structural changes caused by the incorporation of the secondary phase during coating

---

*Corresponding author. Tel.: +65-790-5526; fax: +65-791-1859.
E-mail address: mkakhor@ntu.edu.sg (K.A. Khor).

formation or the pure existence of the additives to alter coating properties. A good understanding of the composite coating formation mechanism and structure characterization could contribute considerably to the development of the composite bioceramic coatings. So far, most of the work has been conducted on bulk composite materials, aiming to reveal the strengthening mechanism, which mostly includes load transfer model and matrix strengthening model [16]. However, for thermal sprayed coatings, the reinforcing mechanism could be different from that of the bulk composite materials due to the identified inhomogeneous-layered structure and possible chemical reaction between components.

In the present study, the formation mechanism of high velocity oxy-fuel (HVOF) sprayed HA/TiO_2 composite coatings was analyzed using an impact theory. Mutual chemical reaction behavior among the phases present was investigated and the composite structure was characterized through X-ray diffraction (XRD), differential scanning calorimetry (DSC) and transmission electron microscopy (TEM).

2. Experimental details

2.1. Coating preparation

The starting HA powder with a fully crystallized structure $(Ca_{10}(PO_4)_6(OH)_2)$ was prepared by heat treating the spray-dried powder in an electric-resistance furnace at $900°C$ with a duration of 1.5 h. The anatase TiO_2 powder with a mean size of 1 μm was used. Fig. 1 shows the size distribution of the starting powder. The mean particle size of HA was 40 μm. The composite powder was prepared through a mechanical-blending process in a planetary mill (P5, Fritsch GmbH, Germany). A fully computerized HV2000 HVOF system (Praxair Thermal Spray, IN, USA) with a nozzle diameter of 19 mm was employed for the coating deposition on sandblasted Ti–6Al–4 V substrate surface. The fuel gas was hydrogen and the powder carrier gas was argon. The flow rate of oxygen, hydrogen and argon was 283, 566 and 19 l/min, respectively. The flow rates were sustained using mass flow meters. The spray distance was kept at 250 mm by a robotic manipulator arm. The powder feed rate was fixed at 6 g/min with the aid of a computerized powder feeder station.

2.2. Testing methods

The coating microstructure was analyzed using low vacuum scanning electron microscopy (SEM, JEOL JSM-5600LV) and transmission electron microscopy (TEM, JEOL, JEM-2010) operating at 200 kV. Differential scanning calorimetry (DSC, Netzsch Thermal
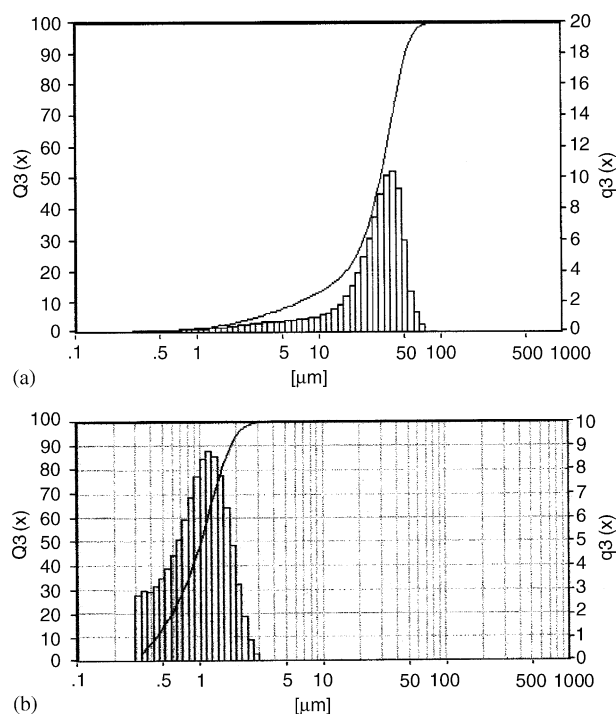

Fig. 1. Particle size distribution of: (a) HA powder, and (b) TiO_2 powder.

Analysis, DSC 404C, Germany) was utilized for the determination of the chemical reaction temperature between HA and TiO_2 and their thermal behavior at elevated temperatures. DSC test used nitrogen gas as the atmosphere with a flow rate of 150 ml/min and the heating and cooling rate was $10°C$/min. The phase composition of the starting powder and as-sprayed coatings was qualitatively analyzed by means of XRD method (MPD 1880, Philips, the Netherlands). The operating conditions were 40 kV and 30 mA by using Cu $K_α$ radiation. The goniometer was set at a scan rate of $0.015°$/s over a $2θ$ range 20–80°. Fourier transform infrared (FTIR, Nicolet Magna FTIR-560) spectroscopy analysis was performed to characterize the changes of ion groups in the materials. The infrared spectrum with a resolution of $4 cm^{-1}$ and the scan number of 100 was adopted with a scan range $400–4000 cm^{-1}$.

3. Impact formation of the composite coatings

Fig. 2 shows the typical surface morphology of the HVOF composite coating. The SEM image together with EDX analysis reveals that the TiO_2 powder was not melted during coating formation. It is widely believed that the flattening procedure of individual sprayed particles is isolated and the flattening terminated before the impingement of subsequent particle, so the cohering
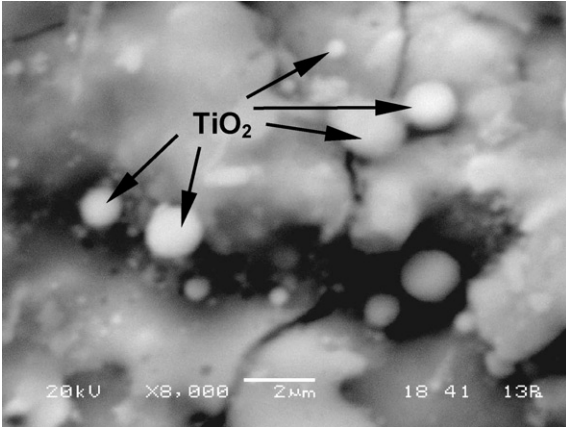
Fig. 2. Typical surface morphology of the as-sprayed composite coating (HA + 20 vol% TiO$_2$) showing the bright small TiO$_2$ spheres.
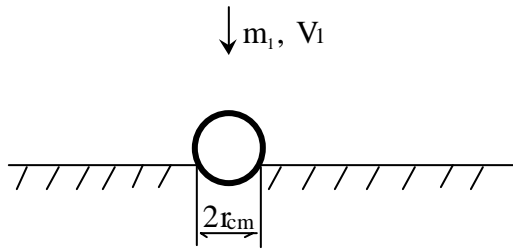

Fig. 3. Sketch of impact of TiO$_2$ particle upon HA splat matrix.

process of the reinforcements to HA matrix can be treated as impact of solid spherical particle upon solid surface. In the present study, compared to HA splat dimension, the titania particle is of very small size, thus it can be treated as the impact of a sphere onto a static flat surface. The schematic illustration of the impact procedure is shown in Fig. 3. The physical properties of both HA and TiO$_2$ used in the present study are Young's modulus: HA-30 GPa [17], titania-282 GPa, and Poisson ratio: HA-0.28 [18], titania-0.278, respectively.

Assuming that impact process of the two solids can be regarded as quasi-static elastic impact of frictionless materials, the contact is known as the Hertzian contact. From the contact analysis of two spheres, the pressure distribution (Hertz pressure distribution), in which the pressure at any location within the contact area is represented, is presented as follows [19]:

$$p(r) = \frac{3}{2} \frac{F_z}{\pi r_c^3} (r_c^2 - r^2)^{1/2}, \tag{1}$$

where F_z is the total loading force, which can be obtained from Newton law, $m_1(\mathrm{d}V_1/\mathrm{d}t) = -F_z$, where m_1 and V_1 are the mass and velocity of the impact particle shown in Fig. 2, respectively, r_c is the maximum radius of contact surface. Concerning that the matrix is flat, it was derived that [19,20]

$$\alpha = \frac{3F_z}{4E^* r_c}; \quad \frac{3F_z}{4E^* r_c^3} = \frac{1}{R}, \tag{2}$$

where α is the approaching distance of the center of TiO$_2$ particle, hence the deformation depth along vertical direction under Hertzian force. R is the radius of TiO$_2$ particle. E^* is the contact modulus defined by Brach [20]

$$\frac{1}{E^*} = \frac{1 - v_1^2}{E_1} + \frac{1 - v_2^2}{E_2}. \tag{3}$$

Then the pressure distribution becomes

$$p(r) = \frac{3}{2\pi} \left(\frac{16}{9} F_z \frac{E^{*2}}{R^2} \right)^{1/3} \left[\left(\frac{3}{4} F_z \frac{R}{E^*} \right)^{2/3} - r^2 \right]^{1/2}. \tag{4}$$

Combining Eq. (2) with the Newton's law, $(\mathrm{d}^2\alpha/\mathrm{d}t^2) = -F_z(1/m_1)$, following formula can be derived

$$\frac{\mathrm{d}^2\alpha}{\mathrm{d}t^2} = -\frac{4}{3} \frac{E^*}{m_1} \sqrt{R} \alpha^{3/2}. \tag{5}$$

The initial conditions are given by

$$\left(\frac{\mathrm{d}\alpha}{\mathrm{d}t} \right)_{t=0} = V_1; \ \alpha_{t=1} = 0. \tag{6}$$

Multiplying both sides of Eq. (5) by $\mathrm{d}\alpha/\mathrm{d}t$ yields

$$\frac{\mathrm{d}\alpha}{\mathrm{d}t} = \left(V_1^2 - \frac{16}{15} \frac{E^*}{m_1} \sqrt{R} \alpha^{5/2} \right)^{1/2}. \tag{7}$$

Since the maximum deformation occurs at $\mathrm{d}\alpha/\mathrm{d}t = 0$, thus

$$\alpha_m = \left(\frac{15}{16} \frac{m_1 V_1^2}{E^* \sqrt{R}} \right)^{2/5}. \tag{8}$$

Then the maximum radius of the collision contact area can be given by

$$r_{cm} = \sqrt{R} \left(\frac{15}{16} \frac{m_1 V_1^2}{E^* \sqrt{R}} \right)^{1/5}. \tag{9}$$

The impact duration can also be obtained from Eq. (7)

$$t_c = \frac{2.94}{V_1} \left(\frac{15}{16} \frac{m_1 V_1^2}{E^* \sqrt{R}} \right)^{2/5}. \tag{10}$$

Since the composite coating formation prevails, it can be assumed that the velocity of the particle at the end of the impact approaches zero, in other word, no rebounding occurs.

The impact duration/crater radius versus titania particle diameter is shown in Fig. 4 with the titania particle velocity assumed as 400 m/s. It is found that the impact duration corresponds with the increase of titania particle size, and the crater radius changes in similar manner. The impact duration, hence the composites forming duration, is less than 1 μs as the titania particle diameter is around 1 μm. It is noted that the diameter of the crater induced by the impact is far smaller that that of TiO$_2$ particle, which is around one-second of the particle size. This indicates that the TiO$_2$ particle cannot possibly produce the crater with a diameter equal to its
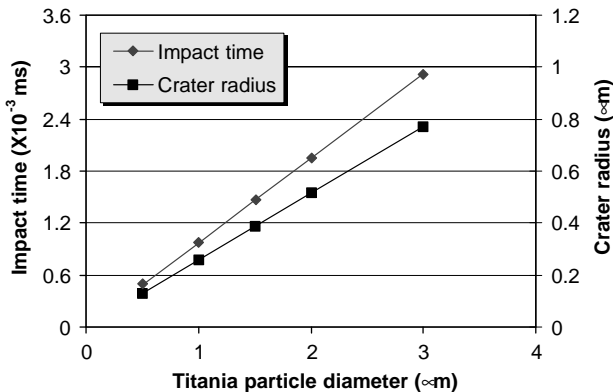
Fig. 4. Effect of titania particle size on impact duration and crater radius with the assumption that the particle impinging velocity is 400 m/s.

Fig. 5. XRD patterns of the HVOF sprayed: (a) pure HA coating, and (b) HA + 20 vol% TiO_2 composite coating.

own dimension. It was reported that the crater should be at least equal to the size of the reinforcing particle for the sake of entrapment [21]. However, that report did not consider other possible factors, such as chemical reaction, and crack formation. Even provided that no flaws appear and no mutual reaction with the matrix occurs, the inelastic procedure can also more or less absorb the impact energy, thus effectively avoid rebounding. Therefore, the critical crater size (defined here as the size at which value the powder can be trapped with matrix together) can be effectively decreased. The small crater size indicates that, in addition to the mechanical interlocking induced by the crater, other factors should contribute to the cohesion of the splats.

4. Mutual chemical reaction between HA and titania

The XRD patterns of the as sprayed HA and HA/ TiO_2 coatings are shown in Fig. 5. It is found that apart from α-TCP and CaO, which resulted from thermal decomposition of HA during coating deposition [22], $CaTiO_3$ is present in the as-sprayed composite coatings. Meanwhile, the trace of rutile TiO_2 points to apparent transformation of anatase TiO_2 to rutile at high temperatures. The following chemical mutual reaction is believed to have occurred during the composite coating formation:

$$Ca_{10}(PO_4)_6(OH)_2 + TiO_2 \rightarrow 3Ca_3(PO_4)_2 + CaTiO_3 + H_2O. \tag{11}$$
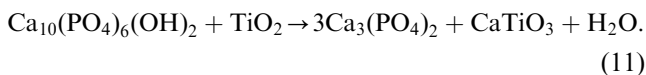
Regarding the unmelted state of the titania particles shown in Fig. 2, it is believed that some anatase titania transforms to rutile and the rest reacts with HA. A previous study found that HA prefers to react chemically with anatase than rutile [11]. The mutual chemical reaction behavior was further investigated by using the high temperature DSC technique. Fig. 6 shows the DSC
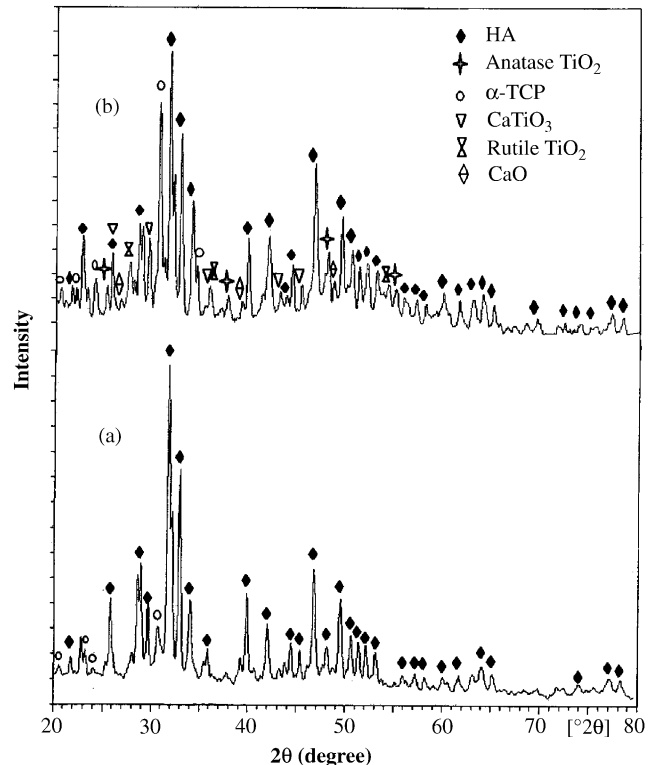
heating curves of the as-sprayed composite coating with the comparison to the starting powder and pure HA coating. The comparison among the mixed powder (c) and pure HA (a) and TiO_2 (b) powder indicates that the mutual chemical reaction occurs at around 1410°C under the present DSC conditions. The subsequent endothermic peak labeled at around 1457°C would be the point where further transformation of remaining HA [17] or oxyapatite [23] occurs. It also indicates that the chemical reaction takes place while the components are in solid state. The large broad peak demonstrated by HA powder, which is labeled from around 1200°C to 1340°C shown in Fig. 6(a), suggests the dehydration of HA over a wide temperature range and phase transformation of HA to oxyhydroxyapatite (OHAP, $Ca_{10}(PO_4)_6(OH)_{2-x}O_x$ $_x$) [24]. It is found that the incorporation of TiO_2 effectively inhibits this dehydration procedure. The DSC curve corresponding to the composite coating, curve (e) in Fig. 6, virtually shows the same thermal behavior as the pure HA coating (curve (d)). However, there is still a limited peak marked at around 1410°C for the composite coating, which indicates further mutual chemical reaction. Given that thermal spray is a rapid solidification process, the cooling rate of splats could be up to 10^6 K/s, according to the impact duration shown in Fig. 4, which is usually less than 2 μs, it is believed that the chemical reaction

could take place during the impinging process. Once the impact completes, the reaction should naturally terminate. Bearing in mind the considerable amount of titania in the composite coating, the very limited peak demonstrated at around 1410°C indicates that once the surrounding part of titania particle reacts with HA during coating formation, the reaction products present around titania particles can effectively inhibit further mutual reaction. The peak labeled at around 1021°C for the pure HA coating and 1088°C for the composite coating could be the temperature at which point reversible reaction from TCP to HA occurs [25].

In order to further reveal the thermal behavior of the samples at elevated temperatures, DSC cooling curves was also studied, which are demonstrated in Fig. 7. It is found that, for pure HA, only one visible peak appears, which is around 1440°C, and it may refer to the reversed

full phase transformation from unstable $\bar{\alpha}$–TCP to α–TCP [23]. The $\bar{\alpha}$–TCP may come from the transformation of α–TCP at elevated temperatures [23]. Owing to the lacks of water in the pure nitrogen atmosphere, no peaks referring to reversible transformation from TCP or TTCP to oxyapatite or HA are present, which was revealed by other researchers using air circumstance [24]. However, for the HA/titania composites, a secondary peak is demonstrated at around 1339°C for the powder and 1320°C for the coating besides the peak labeled at 1414°C and 1457°C referring to the same phase changes as HA. In order to identify the peak representation, DSC heating and cooling was performed for several times for the same starting composite powder. Result shows that the secondary exothermic peaks all present at approximately the same temperature point, which indicates that the peak could represent
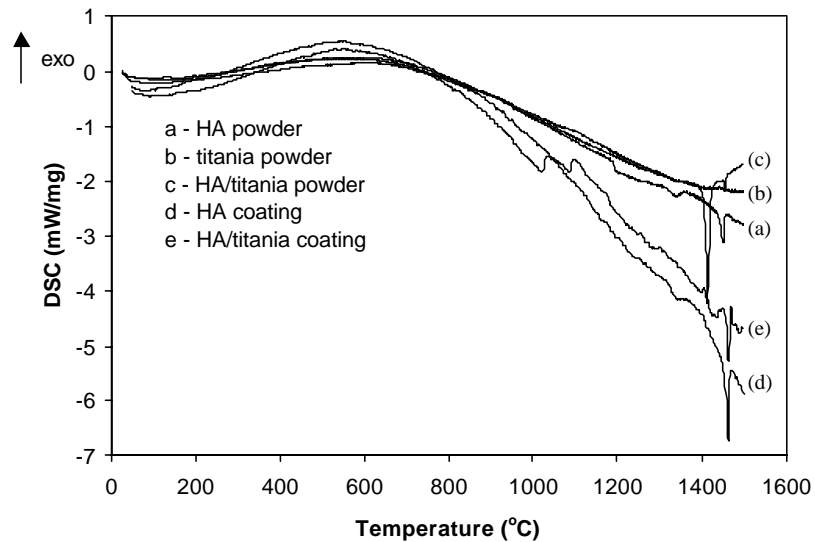

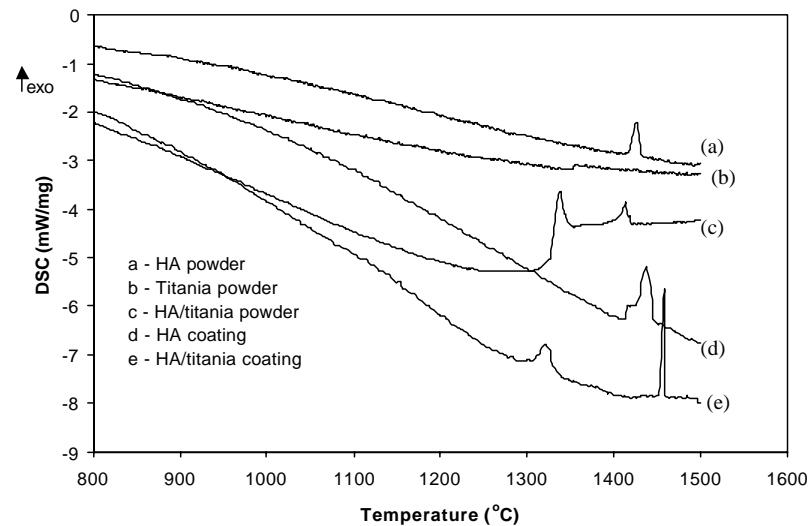Fig. 6. DSC heating curves of the investigated samples.

Fig. 7. DSC curves of the investigated samples showing different behaviors during cooling.

further deferred phase transformation in the HA family triggered by the existence of $CaTiO_3$ and/or titania.

FTIR spectra of the HA/titania composites, before and after coating deposition, are shown in Fig. 8. The weakening of the peak labeled at $3570\,cm^{-1}$ (assigned to the stretching mode of hydroxyl (OH^-) group in HA) in as-sprayed composite coating compared to the starting powder confirms what the XRD result indicated, that is, some of the HA reacted chemically with titania while the rest decomposed during HVOF coating formation. Both procedures triggered decreased content of crystalline HA. The disappearance of the band at $630\,cm^{-1}$ (derived from the hindered rotation mode of OH^- group in HA) further confirms the phase transformation of HA to TCP. The stretching vibration bands of PO_4^{3-} labeled at 958 and $1091\,cm^{-1}$ are observed in both the samples. However, in the composite coating, the resolution diminishes, which may suggest the relative content of the vibration mode group. The peaks labeled

at 569 and $600\,cm^{-1}$ indicate the bending mode PO_4^{3-}. The changes of PO_4^{3-} are thus revealed.

Fig. 5 demonstrates that $CaTiO_3$ forms during the HVOF coating process as a result of the mutual chemical reaction between HA and TiO_2. For the purpose of disclosing at which stage the mutual reaction occurs, HVOF spheroidized composite powder was collected through spraying into distilled water, and subsequently filtered out and dried. The XRD result showed no trace of $CaTiO_3$, confirming that the mutual chemical reaction takes place during the impingement stage. As the tensile failure always occurs within coating rather than at the coating/substrate interface which suggesting the importance of cohesion [22], the chemical reaction between HA and titania should play some important roles in influencing coating mechanical properties.

5. Structure characterization

In order to reveal the detailed structure of the HA/titania composite coatings, SEM and TEM observation was conducted on cross-sections of the composite coatings. Typical HA/titania composite structure is shown in Fig. 9(a). Fig. 9(b) demonstrates the magnified view of the HA/titania interface, which further reveals the bright interface zone with a width of around 140 nm. It is obvious that the interface zone is highly dense. The EDX analysis reveals the approximate elemental atomic ratio of Ti to Ca across this area, which is shown in Fig. 10. It can be stated that the surrounding white ring is composed mainly of the chemical reaction products. The altered ratios further indicate the presence of a mixture of TCP and $CaTiO_3$. It is found that the reaction takes place mainly at the intimate contact area between HA and titania and owing to the temperature
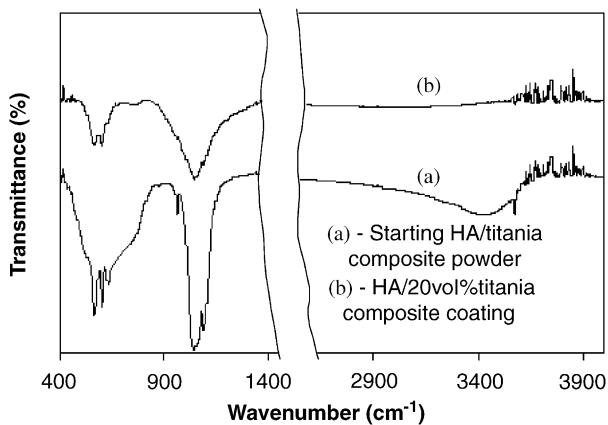

Fig. 8. IR spectra of (a) starting HA/titania composite powder and (b) HA/titania composite coating showing the changes of ion groups after coating deposition.
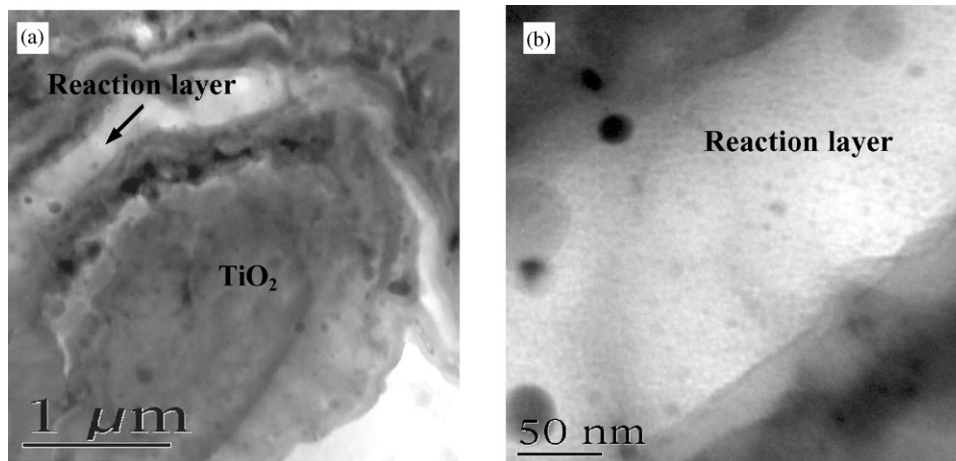

Fig. 9. Morphology of the HA/titania composite structure showing (a) titania is surrounded by a chemical reaction layer, and the enlarged bright interface zone, and (b) showing that the reaction layer has a thickness of around 140 nm.

limit, which is required for the reaction, the reaction terminates once the cooling of the splats prevails.

The morphology comparison between the composite coating and pure HA coating shows difference in HA grain size, which is demonstrated in Fig. 11. It is found
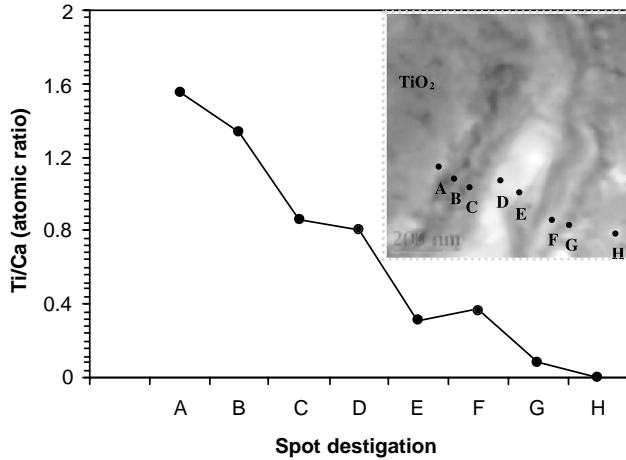

Fig. 10. Ti/Ca atomic ratios corresponding to the altered spot locations marked in the image, the detecting spot is of the size of $25 \, \text{nm}^{-1}$.

that, near the HA/titania interface zone, the HA grain size is larger than those in corresponding pure HA coating. This could be attributed to the decreased thermal diffusion induced by the mutual reaction layer between HA and titania. Moreover, as indicated in Fig. 9, α-TCP resulted from the chemical reaction is of far smaller grain size than those resulted from HA phase decomposition at elevated temperatures, which is shown in Fig. 12. It was reported that the fine grain is beneficial for the improvement of fracture toughness of HA [26]. Especially for thermal sprayed coating, the splats' interface always plays a remarkable role in property determination [27], the fine grains located at HA/titania splats' interface could be beneficial for property improvement of the HA coatings. In the previous report [22], a partial-melted state of HA particles was disclosed during HVOF spraying. The present study claims the influence of TiO_2 incorporation on resolidification process of the partial-melted HA powder during flattening.

Generally, owing to the special formation mechanism, thermal sprayed coating shows an inhomogeneous structure, which contains many defects, such as pores, cracks, etc. For pure HA coating, pure mechanical
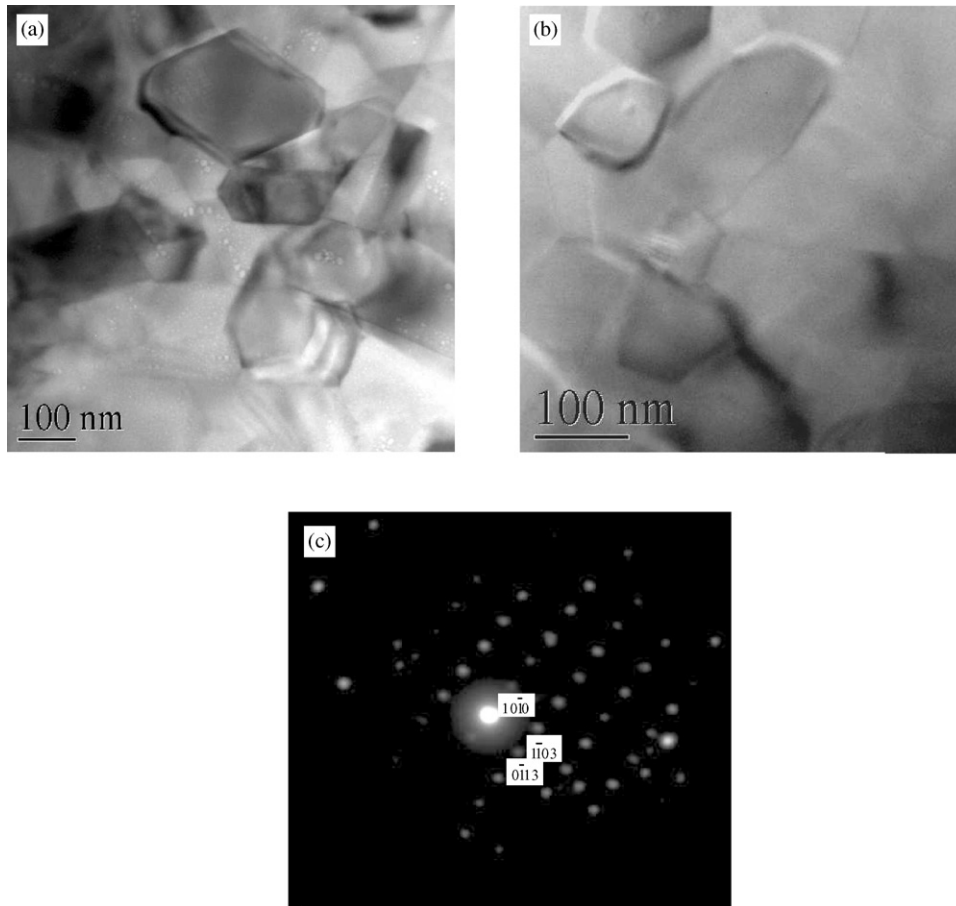

Fig. 11. TEM images showing HA grains in the composite coating near HA/titania interface (a) and pure HA coating (b). Coarsened HA grains in the composite coating are revealed. (c) A selected area diffraction pattern of HA crystal from [$\bar{1} 2 \bar{1} 1$] zone axis.
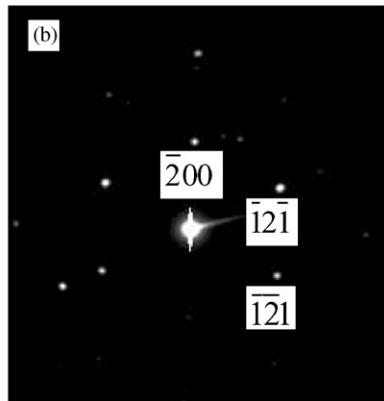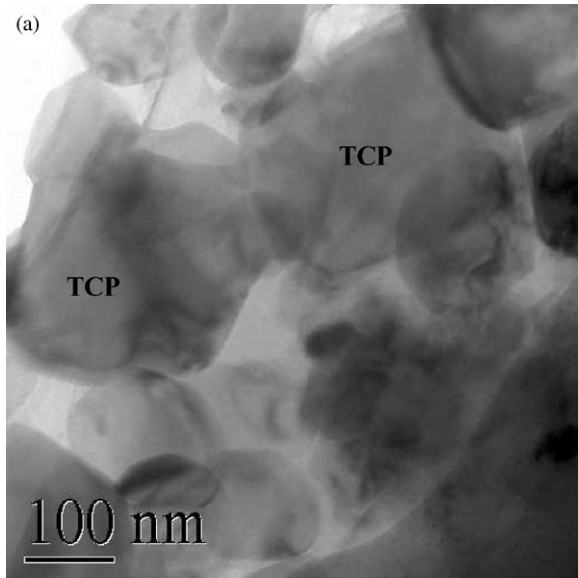
Fig. 12. TEM image of α-TCP grains with large grain sizes (a), (b) [0 1 2] zone selected area diffraction pattern of α-TCP.

Fig. 13. Schematic illustration of the HA/titania composites showing the approximate locations of different phases.

interlocking among HA splats may be the main bonding mechanism. While for the HA/titania composite coatings investigated in the present study, a chemical bond is suggested. From the coating morphology shown in Fig. 9, improved coating structure in terms of decreased porosity could be claimed. This point was confirmed by SEM cross-sectional morphology observation. The defects within the coatings, mostly located among splats, can be chemically healed to some extent by the chemical reaction resultants. It has been pointed out that coating microstructure acted as an important factor in determining the fracture property or even failure location during fracture test of the thermal sprayed coatings [27,28]. It deems that the mutual chemical reaction between the two components supplies higher density, which was believed as one beneficial factor towards improving the fracture property [28].

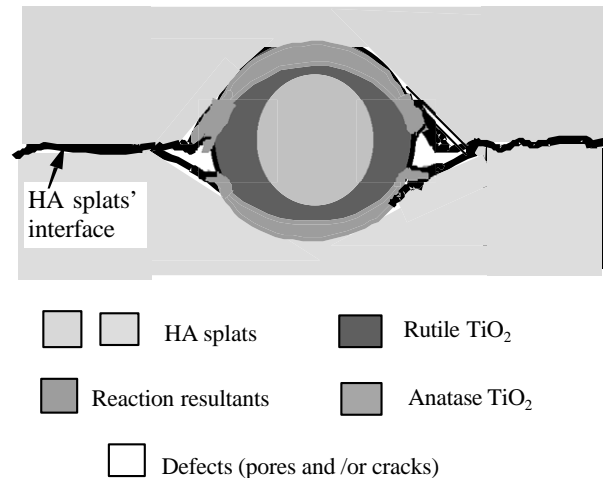It should be noted that the chemically resulted $CaTiO_3$ is not bioactive compared to the phases in HA family. However, since calcium phosphate coatings dissolve after extended implantation periods [29], the chemical bonding between HA/titania splats resulted from the mutual reaction may be beneficial for the prevention of release of titania particles into surrounding tissue or release of these particles as wear products that can lead to prosthesis rejection. Moreover, the TiO_2 is a very stable while bioactive material in bony tissue, and thus can also be effectively used to prevent release of substrate alloy to the surroundings [30]. Furthermore, the existence of TiO_2 can supply high strength and HA impregnating could, on the other hand, increase the bioactivity of the TiO_2 [31].

Regarding the results obtained in the present study on the HA/TiO_2 composite coatings, a structure model, which is shown in Fig. 13, can be proposed to approximately demonstrate the different phase locations within the composite structure. Concerning the impact time consumed for the composite structure formation, the chemical reaction between HA and TiO_2 needs to be further studied using a thermodynamics theory.

6. Conclusion

An impact theory was utilized to logically explain the HA/titania composite coating formation and the mutual chemical reaction between HA and titania during HVOF spraying was analyzed. It was found that the crater caused by the impingement of completely unmelted TiO_2 particles upon HA matrix was of far smaller size than the incipient size of the titania particles. A chemical bond between HA and TiO_2 within the composite coatings was suggested, which may be responsible for the entrapment of titania particles during the impingement process. DSC analysis revealed that the reaction between HA and titania occurred at

around 1410°C and the co-existence of titania influenced the thermal behavior of HA during both heating and cooling cycles. It was found that the mutual reaction between the mechanically blended components took place during the impingement stage. The reaction zone and phase locations in the HA/titania composite coatings were identified through TEM observation. This study revealed that the reaction product present around TiO$_2$ particulates was beneficial for the improvement of the coating structure. Furthermore, the chemical reaction between the components shows some influence on the grain growth of HA during its resolidification. This is believed to be consequential towards the mechanical properties and biological behaviour of the composite coatings.

References

[1] Haman JD, Chittur KK. Four point bend testing of calcium phosphate coatings. Proceedings of the 16th Southern Biomedical Engineering Conference, 1998. p. 305–8.

[2] Kangasniemi IMO, Verheyen CCPM, van der Velde EA, de Groot K. In vivo tensile testing of fluorapatite and hydroxylapatite plasma-sprayed coatings. J Biomed Mater Res 1194;28:563–72.

[3] Yang CY, Wang BC, Lee TM, Chang E, Chang GL. Intramedullary implant of plasma-sprayed hydroxyapatite coating: an interface study. J Biomed Mater Res 1997;36:39–48.

[4] Wang S, Lacefield WR, Lemons JE. Interfacial shear strength and histology of plasma sprayed and sintered hydroxyapatite implants in vivo. Biomaterials 1996;17:1965–70.

[5] Suchanek W, Yashima M, Kakihana M, Yoshimura M. Hydroxyapatite ceramics with selected sintering additives. Biomaterials 1997;18:923–33.

[6] Labat B, Chamson A, Frey J. Effects of r-alumina and hydroxyapatite coatings on the growth and metabolism of human osteoblasts. J Biomed Mater Res 1995;29:1397–401.

[7] Gautier S, Champion E, Bernache-Assollant D. Toughening characterization in alumina platelet-hydroxyapatite matrix composites. J Mater Sci Mater Med 1999;10:533–40.

[8] Lopes MA, Santos JD, Monteiro FJ, Knowles JC. Glass-reinforced hydroxyapatite: a comprehensive study of the effect of glass composition on the crystallography of the composite. J Biomed Mater Res 1998;39:244–51.

[9] Knowles JC, Talal S, Santos JD. Sintering effects in a glass reinforced hydroxyapatite. Biomaterials 1996;17:1437–42.

[10] Yamada Y, Watanabe R. Effect of dispersed pores on fracture toughness of Hap/PSZ composites. Scripta Mater 1996;34:387–93.

[11] Weng J, Liu X, Zhang X, Ji X. Thermal decomposition of hydroxyapatite structure induced by titanium and its dioxide. J Mater Sci Lett 1994;13:159–61.

[12] Vu TA, Heimann RB. Influence of the CaO/TiO$_2$ ratio on thermal stability of hydroxyapatite in the system Ca$_5$(PO$_4$)$_3$OH–CaO-TiO$_2$. J Mater Sci Lett 1997;16:1680–2.

[13] Li J. Behaviour of titanium and titania-based ceramics in vitro and in vivo. Biomaterials 1993;14:229–32.

[14] Webster TJ, Siegel RW, Bizios R. Osteoblast adhesion on nanophase ceramics. Biomaterials 1999;20:1221–7.

[15] Blum J, Eckert KL, Schroeder A, Petitmermet M, Ha SW, Wintermantel E. In vitro testing of porous titanium dioxide ceramics. In: Tadashi Kokubo, Takashi Nakamura, Fumiaki Miyaji, editors. Bioceramics, Vol. 9, Proceedings of the 9th International Symposium on Ceramics in Medicine. Utsu, Japan, 1996, p. 89–92.

[16] Ranganath S. A review on particulate-reinforced titanium matrix composites. J Mater Sci 1997;32:1–16.

[17] Hideki A. Medical applications of hydroxyapatite. Tokyo, st. Louis: Ishiyaku EuroAmerica, 1994.

[18] Ravaglioli A, Kraejewski A. Bioceramics: materials, properties and applications. London: Chapman & Hall, 1992.

[19] Fan LS, Zhu C. Principles of gas-solid flows. Cambridge: Cambridge University Press, 1998.

[20] Brach RM. Mechanical impact dynamics, rigid body collisions. New York: Wiley, 1991.

[21] Tiwari R, Herman H. Development of composite microstructures by thermal spraying. Proceedings of the fourth National Thermal Spray Conference. Pittsburgh, PA, USA, 1991:375–80.

[22] Li H, Khor KA, Cheang P. Effect of the powders' melting state on the properties of HVOF sprayed hydroxyapatite coatings. Mat Sci Eng A 2000;293:71–80.

[23] Zhou J, Zhang X, Chen J, Zeng S, de Groot K. High temperature characteristics of synthetic hydroxyapatite. J Mater Sci Mater Med 1993;4:83–5.

[24] Liao C, Lin F, Chen K, Sun J. Thermal decomposition and reconstitution of hydroxyapatite in air atmosphere. Biomaterials 1999;20:1807–13.

[25] Vogel J, Russel C, Guntheer G. Characterization of plasma-sprayed hydroxyapatite by P-MAS-NMR and the effect of subsequent annealing. J Mater Sci Mater Med 1996;7: 495–9.

[26] Van Landuyt P, Li F, Keustermans JP, Streydio JM, Delannay F, Munting E. The influence of high sintering temperatures on the mechanical properties of hydroxylapatite. J Mater Sci Mater Med 1995;6:8–13.

[27] Callus PJ, Berndt CC. Relationships between the mode II fracture toughness and microstructure of thermal spray coatings. Surf Coat Technol 1999;114:114–28.

[28] Shaw LL, Barber B, Jordan EH, Gell M. Measurements of the interfacial fracture energy of thermal barrier coatings. Scr Mater 1998;39:1427–34.

[29] Hirofumi Kido DDS, Saha S. Effect of HA coating on the long-term survival of dental implant: a review of the literature. J Long-Term Effects of Medical Implants 1996;6:119–33.

[30] Kurzweg H, Heimann RB, Troczynski T, Wayman WL. Development of plasma-sprayed bioceramic coatings with bond coats based on titania and zirconia. Biomaterials 1998;19:1507–11.

[31] Li P, Groot K, Kokubo T. Bioactive Ca$_{10}$(PO$_4$)$_6$(OH)$_2$–TiO$_2$ composite coating prepared by sol-gel process. J Sol–Gel Sci Technol 1996;7:27–34.